www.nature.com/cr
www.cell-research.com

LETTER TO THE EDITOR

Structure of the mannose transporter of the bacterial phosphotransferase system

Cell Research (2019) 29:680–682; https://doi.org/10.1038/s41422-019-0194-z

Dear Editor,

The bacterial phosphoenolpyruvate (PEP): sugar phosphotransferase system (PTS) mediates the active transport and concomitant phosphorylation of carbohydrates.[1] The PTS comprises two cytoplasmic phosphoryl proteins (*i.e.*, EI and HPr) and a species-dependent variable number of sugar-specific EII complexes (including IIA, IIB, and membrane-embedded subunits IIC/IID). EI and HPr transfer phosphoryl groups from PEP to the IIA unit. IIA and IIB sequentially transfer phosphates to sugar, which is translocated by the IIC/IID unit.[2] Bacterial PTSs are classified into four evolutionarily distinct (super) families: (i) glucose/fructose/lactose (GFL) superfamily, (ii) ascorbate/galactitol (AG) superfamily, (iii) mannose–fructose–sorbose family (man-PTS), and (iv) non-transporting dihydroxyacetone family. The crystal structures of IIC transporters from GFL and AG superfamilies have been reported previously.[3,4] All IIC proteins from GFL and AG superfamilies are homodimers and use an elevator mechanism to transport substrates across the cell membrane. However, the mannose family is unique in several aspects among the PTS families.[1] The mannose family is the only PTS family whose members possess a IID protein, and its IIC and IID subunits have evolved in parallel and are unstable when expressed separately.[2] The mannose family is also the only member among the PTS families in which the IIB constituent is phosphorylated on a histidine residue rather than a cysteine residue.[3] In addition to its function in carbohydrate uptake and phosphorylation, the membrane-located components of the man-PTS complex exhibit two additional apparently unrelated activities: they play a role in the infection of *Escherichia coli* by bacteriophage λ for DNA penetration in the inner membrane, and they serve as target receptors for class IIa, IId, and IIe bacteriocins. Notably, class IIa and IId bacteriocins have attracted attention as potent narrow-spectrum alternatives to antibiotics or as food preservatives.[5] In this study, we report the cryo-EM structure of *E. coli* man-PTS at resolution of 3.52 Å, which comprises ManY and ManZ, corresponding to IIC^{Man} and IID^{Man} components, respectively (Supplementary information, Fig. S1 and Table S1). The high quality of the ManYZ EM density allowed us to perform de novo model building for ManY and ManZ (Supplementary information, Fig. S2).[6]

The structure of ManYZ, trapped in an inward-facing conformation, reveals a three-fold symmetry axis perpendicular to the membrane (Fig. 1a). The trimer has dimensions of ~104 Å × 104 Å × 73 Å (Fig. 1a, b). Each protomer is composed of a ManY and ManZ, which have a similar fold and are related to each other by a pseudosymmetry axis parallel to the membrane (Supplementary information, Fig. S3). ManY consists of nine transmembrane helices (TM1–9Y) and one horizontal periplasmic amphipathic α-helix (AH1Y), with N- and C-termini on periplasmic and cytoplasmic sides, respectively (Fig. 1c). ManZ also contains nine transmembrane helices (TM1–9Z) and two horizontal amphipathic α-helices (AH1Z and AH2Z), with N- and C-termini on cytoplasmic and periplasmic sides, respectively (Fig. 1d). However, TMs 1–6Z are located on the cytoplasmic side of the membrane in this inward-facing conformation (Fig. 1d). ManYZ oligomerization is mediated entirely by extensive interactions between two C-terminal TMs (TM8Y and TM9Y) of ManY (Fig. 1b), mostly through hydrophobic residues. According to their structures, ManY and ManZ can be classified as CoreY, ArmY, and VmotifY and CoreZ, ArmZ, and VmotifZ domains, respectively (Fig. 1e). VmotifY and VmotifZ interlock to form the Vmotif domain of the complex (Fig. 1f). CoreY and CoreZ clamp the substrate to form the Core domain (Supplementary information, Fig. S4a). The helices AH1Y and AH1Z are designated as ArmY and ArmZ domains. ManY and ManZ have similar folds and can be topologically superimposed (Supplementary information, Fig. S3). However, once ManY and ManZ are aligned solely according to their CoreY and CoreZ domains, VmotifY and VmotifZ domains swing apart due to different orientations of ArmY and ArmZ (Fig. 1g). When ManY and ManZ are aligned according to the Vmotif domain, the Core domains rotate in the membrane (Fig. 1h), which is assumed to be the root of the elevator mechanism model of transport.[7]

The mannose transporter of *E. coli* has a broad substrate specificity, including glucose, mannose, fructose, glucosamine, N-acetylglucosamine, and N-acetylmannosamine, and it is the only transporter for mannose.[8] In the cryo-EM map, the ManYZ structure has a pie-shaped non-protein density corresponding to a bound mannose on each protomer (Supplementary information, Fig. S4b). Similar to the L-ascorbate PTS transporter UlaA, the substrate mannose is caged in an ellipsoid-shaped binding pocket of the Core domain with a volume of ~108.7$Å^3$ (Fig. 1i). The two loops, L12Y and L34Y, of ManY shape the top and left sides of the cleft, whereas loops L12Z and L34Z from ManZ shape the bottom side of the pocket. The right-side wall is mainly constructed of residues from TM5Z (Fig. 1j). The C6 hydroxyl on the substrate can be phosphorylated by IIB, and it orients to the solvent ready for phosphorylation (Fig. 1k). The N65P mutation of ManY, which breaks down the hydrogen bond between the backbone of Asn65 and the substrate mannose, significantly impaired the mannose transport capacity as measured by reconstituted proteoliposome assays (Fig. 1l). A large cavity around OH-2 is supposed to accommodate the acetyl group from derivatives, that is, N-acetylmannosamine and N-acetylglucosamine. However, the man-PTS from *Vibrio furnissii* cannot transport N-acetylglucosamine,[9] possibly because the hydrogen bond between Asp25 and Asn65 is lost due to the replacement of Asp with Gly. The unusually lengthy loop L34Y covers the substrate-binding pocket, and its stability is enforced by the hydrogen bond between Asn65 and the backbone of Val70. Either L34Y loop deletion by the truncation of residues from Asn65 to Val70 or stability disruption by the N65A point mutation destroyed microsomal mannose uptake activity (Fig. 1l).

Based on our structure, we proposed that similar to other PTS IIC transporters, the molecular mechanism of man-PTS "vectorial"

Received: 4 March 2019 Accepted: 14 May 2019
Published online: 17 June 2019

© IBCB, SIBS, CAS 2019

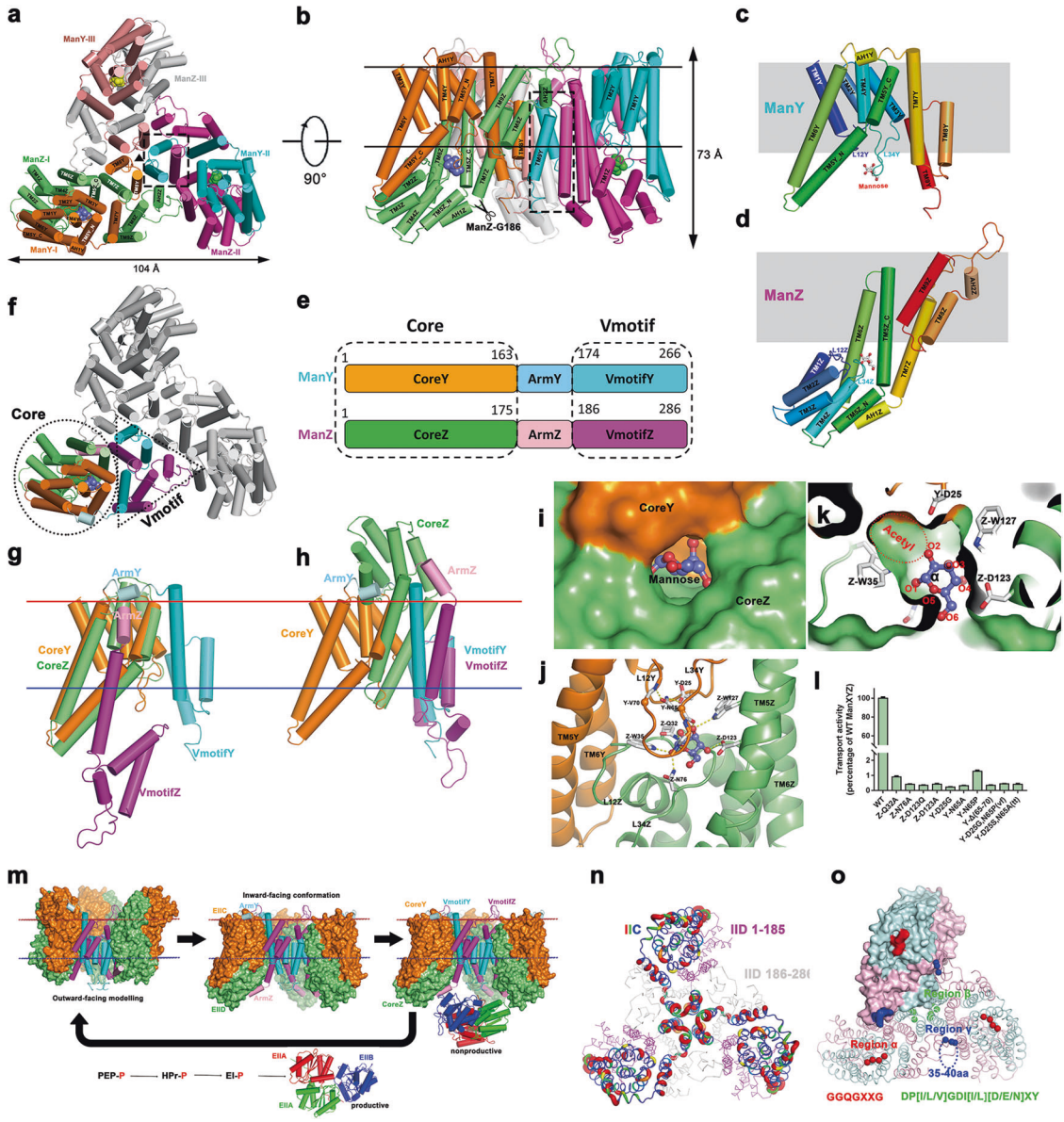

Fig. 1 Cryo-EM structure study of ManYZ complex. **a**, **b** Cartoon representation of the ManYZ structure is shown in two perpendicular views. The scissor in **b** indicates the maximum C-terminal truncation of ManZ, at which the penetration of λ DNA across the inner membranes is only slightly affected. **c**, **d** ManY **c** and ManZ **d** are cartoon-represented and rainbow-colored. **e** Color-coded domain architecture of ManY and ManZ. The same color scheme is used in all structure figures below if not specified elsewhere. **f** The structure of ManYZ complex with domains color-coded as aforementioned. VmotifY and VmotifZ interlocked to form Vmotif domain, whereas CoreY and CoreZ give rise to Core domain. **g** The structure alignment of ManY and ManZ based solely on Core domain. ArmY and ArmZ separate, which induces VmotifY and VmotifZ in the different orientation. **h** Structure alignment of ManY and ManZ based on Vmotif domain. **i**, **j** Surface representation of substrate-binding pocket. **k** Mannose is shown as sticks with carbon in slate and oxygen in red. Protein–mannose interactions are marked as dotted lines. **l** The proteoliposome assay of 15 min D-[2-^{3}H]-mannose uptake for ManYZ variants. Details of the experiments are described in the 'Materials and methods' section in Supplementary information. Error bars are s.e.m of three independent measurements. **m** The elevator mechanism of mannose transportation by ManXYZ complex. Outward-facing model constructed according to the symmetrical roles of ManY and ManZ. CoreY, VmotifY, CoreZ and VmotifZ domains are colored in orange, cyan, lime and magenta, respectively. EIIAs are colored in red and green, and EIIB in blue. **n** The putty representation of non-conservation of ManY/IIC between *E. coli* and *K. pneumoniae*, which is the major specificity determinant for bacteriophage λ infection, is shown and colored in rainbow from blue to red. The residues 186–286 of ManZ/IID are colored gray to indicate that their truncation does not affect the penetration of lambda DNA. However, the residues 1–186 of ManZ, although not specificity determinant, are colored in magenta and necessary for the stability of the whole complex. **o** Three regions of the mannose phosphotransferase system (α: red, β: green, and γ: blue) are responsible for specific targeting by class IIa bacteriocins

phosphorylation is deeply rooted in the symmetry of ManY and ManZ, suggesting a possible elevator mechanism of membrane transport. The transport activity of ManYZ may involve four sequential steps (Fig. 1m). The default state is likely an outward open state (modeled according to the pseudosymmetry between ManY and ManZ). In this state, the CoreZ domain (lime) approaches the VmotifZ domain (magenta). Then, the binding of the substrate to the pocket of the Core domain causes a switch to an inward-facing state through the movement of the Core relative to Vmotif. In this inward-facing state, CoreY (orange) is close to the VmotifY domain (cyan), and the substrate pocket is accessible from the cytoplasmic side. In the third step, IIB transfers the

phosphate anion to mannose coupled with energy. The resultant product, mannose-6-P, might leave the binding site and enter the cytosol. Finally, using the energy coupled with the phosphate originally transferred from PEP, the Core domain returns to the default state, and the whole system restarts this novel cycle of transport.

Bacteriophage DNA has to cross two membranes to reach the cytoplasm of a gram-negative host.[10] The $IICD^{Man}$ (here, ManYZ) complex is required for the penetration of bacteriophage λ DNA across the cytoplasmic membrane of gram-negative bacteria,[11] for example, *E. coli* and *Bacillus subtilis*; however, the $IICD^{Man}$ complex from *Klebsiella pneumoniae* lacks the bacteriophage DNA injection function. The results of a DNA penetration assay suggested that IIC is the major determinant for lambda infection, and >100 residues C-terminal truncation of IID still supports lambda DNA penetration.[12] Comparing the sequences between the IICs of *E. coli* and *K. pneumoniae* (Fig. 1n) revealed that the non-conserved regions are mainly located around the oligomerization interface, which may be the lambda DNA tunnel for bacteriophage infection. From a structural point of view, the absence of fewer than 100 residues from the IID C-terminus (scissor in Fig. 1b, gray thine line in Fig. 1n) would not affect the oligomer state and completeness of the ManYZ complex, which renders the complex capable of DNA penetration. However, the actual role of ManYZ in DNA injection remains unclear.

The antibiotic activity of unmodified bacteriocins from gram-positive bacteria likely depends on the $IICD^{Man}$ complex as a specific target, which dissipates the proton motive force of the target cell through pore formation.[13] The man-PTS family is phylogenetically clustered into groups I, II, and III. Only members from group I function as receptors for class IIa and IId bacteriocins.[14] Group I man-PTS has three distinct regions, termed region-α, region-β, and region-γ, which clearly distinguish IIC and IID proteins with good receptor function from those with poor or no receptor function. The three distinct regions important for class IIa and IId bacteriocin reception are identified on the structure (Fig. 1o).[14] Region-α (red in Fig. 1o), an extracellular loop located between TM4Y and TM5Y, is characterized by the conserved sequence GGQGXXG, which is ready for class IIa bacteriocins (Supplementary information, Fig. S5).[15] Region-β (green in Fig. 1o), located at the C-terminal end of IIC proteins, is characterized by the enrichment of glycine residues and the presence of the conserved sequence DP[I/L/V]GDI[I/L][D/E/N]XY. Finally, region-γ (blue in Fig. 1o) designates a loop between AH2Z and TM7Z in IID proteins, whose group I members contain an additional sequence of 35–40 aa that is absent in their counterparts from groups II and III. Region-α (red) and region-γ (blue) are located on the extracellular side of the receptor and might first interact with the cationic hydrophilic N-terminus of the pediocin-like bacteriocin, which then induces the insertion of an amphipathic portion of the bacteriocin into the membrane. Thereafter, the C-terminus of the bacteriocin might interact with region-β (green), which is located on the cytoplasmic side of the receptor, to stabilize the pore formed by bacteriocins.

In this study, we have solved the cryo-EM structure of ManYZ at the inward-facing conformational state. Man-PTS transporters use an elevator mechanism for substrate transportation, in which the substrate-binding Core domain can undergo a rigid-body rotation across the cell membrane. Because of the multiple roles of the man-PTS, the structure of ManYZ also sheds light on the need for further research to decipher the bacteriophage λ DNA injection and to develop bacteriocins for safe and efficient applications as food preservatives and novel drugs to fight antibiotic-resistant pathogens.

The cryo-EM map and the structure have been deposited to the Electron Microscopy Data Bank (EMD-9906) and the Protein Data Bank (PDB: 6K1H), respectively.

ACKNOWLEDGEMENTS

We thank Professor Nieng Yan (Princeton) for comments on the manuscript, Dr. Qiang Zhou (Tsinghua) for suggestions on cryo-EM data processing, Dr. Xiaomin Li (Tsinghua) for technical support during EM image acquisition, the Tsinghua University Branch of China National Center for Protein Sciences (Beijing) for providing the cryo-EM facility support, and the computational facility support on the cluster of Bio-Computing Platform (Tsinghua University Branch of China National Center for Protein Sciences Beijing). This work was supported by funds from the Ministry of Science and Technology of China (Grant No. 2016YFA0501103 and 2015CB910104) and National Natural Science Foundation of China (31621092). We thank Dr. Xiaochun Li and Mr. Philip Schmiege (UT Southwestern Medical Center) for comments on the manuscript.

AUTHOR CONTRIBUTIONS

X.L. and J.W. conceived the project. X.L., K.H., and J.Z. designed and performed experiments. J.W. wrote the manuscript.

ADDITIONAL INFORMATION

Supplementary information accompanies this paper at https://doi.org/10.1038/s41422-019-0194-z.

Competing interests: The authors declare no competing interests.

Xueli Liu[1], Jianwei Zeng[1], Kai Huang[1] and Jiawei Wang[1]
[1]*State Key Laboratory of Membrane Biology, Beijing Advanced Innovation Center for Structural Biology, School of Life Sciences, Tsinghua University, 100084 Beijing, China*
These authors contributed equally: Xueli Liu, Jianwei Zeng, Kai Huang.
Correspondence: Jiawei Wang (jwwang@tsinghua.edu.cn)

REFERENCES

1. Kundig, W., Kundig, F. D., Anderson, B. & Roseman, S. *J. Biol. Chem.* **241**, 3243–3246 (1966).
2. Deutscher, J. et al. *Microbiol. Mol. Biol. Rev.* **78**, 231–256 (2014).
3. Cao, Y. et al. *Nature* **473**, 50–54 (2011).
4. Luo, P. et al. *Nat. Struct. Mol. Biol.* **22**, 238–241 (2015).
5. Cotter, P. D., Ross, R. P. & Hill, C. *Nat. Rev. Microbiol.* **11**, 95–105 (2013).
6. Zhou, N., Wang, H. & Wang, J. *Sci. Rep.* **7**, 2664 (2017).
7. Boudker, O. & Verdon, G. *Trends Pharmacol. Sci.* **31**, 418–426 (2010).
8. Plumbridge, J. & Vimr, E. *J. Bacteriol.* **181**, 47–54 (1999).
9. Bouma, C. L. & Roseman, S. *J. Biol. Chem.* **271**, 33468–33475 (1996).
10. Casjens, S. R. & Hendrix, R. W. *Virology* **479**, 310–330 (2015).
11. Scandella, D. & Arber, W. *Virology* **58**, 504–513 (1974).
12. Esquinas-Rychen, M. & Erni, B. *J. Mol. Microbiol. Biotechnol.* **3**, 361–370 (2001).
13. Hechard, Y. & Sahl, H. G. *Biochimie* **84**, 545–557 (2002).
14. Kjos, M., Nes, I. F. & Diep, D. B. *Microbiology* **155**, 2949–2961 (2009).
15. Kjos, M., Salehian, Z., Nes, I. F. & Diep, D. B. *J. Bacteriol.* **192**, 5906–5913 (2010).